



www.seetconf.futminna.edu.ng



www.futminna.edu.ng

Transesterification of waste frying oil to methyl ester using activated carbon supported Mg-Zn oxide as solid-base catalyst

M.A. Olutoye¹, E.J.Eterigho², B. Suleiman³, O.D. Adeniyi⁴, I.A. Mohammed⁵, U. Musa⁶

Department of Chemical Engineering, Federal University of Technology, Minna Nigeria.

¹Corresponding Author: m.olutoye@futminna.edu.ng, 08034059454

Abstract

An activated carbon-supported Mg-Zn catalyst (Mg-Zn/AC) was prepared by using co-precipitation combined with incipient wetness impregnation methods. The catalyst structure was characterized by powder X-ray diffraction (XRD), N₂ adsorption-desorption, Fourier transform infrared spectroscopy (FTIR), its microstructure was studied by the use of scanning electron microscopy (SEM) and the catalytic performance toward synthesis of methyl esters from waste frying oil (WFO) was investigated. The properties studied provided insight into the catalytic performance of the catalyst whereby the large surface area and pore volume of the support facilitated the distribution of metal particles and high dispersion of metals. The optimum reaction conditions were obtained by varying parameters such as methanol to oil ratio, catalyst loading, temperature and time. Under the conditions of reaction time of 5 h, temperature, 150 °C and catalyst dosage of 2.5 wt%, the methyl ester yield of >86% was achieved using 64 g of WFO, 38 g of methanol. The results showed that Mg-Zn/AC catalyst presented efficient activity during the transesterification reaction and is a promising heterogeneous catalyst for the production biodiesel fuel from vegetable oil feedstock.

Keywords: Activated carbon; Mg-Zn oxide supported catalyst; Waste frying oil; Biodiesel; Transesterification

1. INTRODUCTION

The dwindling reserves of fossil fuel and surging prices for the petroleum-based fuels has triggered the pressing needs for renewable energy as sustainable fuel substitute (Singh and Singh, 2010). According to the statistical data reported by the International Energy Agency, a 53% increase in the global energy consumption is foreseen by 2030. The energy consumption is mainly based on fossil fuels which account for 88.1%. At the current production rates, the global proven reserves for crude oil and natural gas are forecasted to last for the next 41.8 and 60.3 years (Ong et al., 2011). Several researches on alternative renewable energy sources, namely solar, wind, hydrothermal, geothermal and

biofuels have been carried out extensively (Cheng et al., 2010; Gnansounou and Dauriat, 2010; Yin et al., 2010).

Biodiesel, produced by Transesterification of vegetable oils, fats and fatty acids is recognized as a new emerging sector in fuel industry, due to the similarity it possesses with the conventional diesel in term of its chemical structure and energy content. Several types of vegetable oils which have been used for the preparation of biodiesel includes palm (Zabeti et al., 2009), sundowner (Granados et al., 2007), rapeseed (MacLeod et al., 2008), Canola (D'Cruz et al., 2007), and soybean (Furuta et al., 2004; Kim et al., 2004; Suppes et al., 2004). Another attraction of biodiesel as diesel fuel is that it is a clean-burning fuel, nontoxic with liquid



www.seetconf.futminna.edu.ng



www.futminna.edu.ng

nature-portability, has higher combustion efficiency, provides low emissions of carbon monoxide, particulate matter, unburned hydrocarbons and zero percent of sulfur content compared to petroleum-based fuel, lower sulfur and aromatic content, higher cetane number and it is biodegradable. Simultaneously, no modification in diesel engine is required as biodiesel is compatible with the existing transportation engine models (Al-Zuhair, 2007; Yung and Gon, 2010; Zhang et al., 2009).

Many researches have been conducted in quest for suitable heterogeneous catalysts that have high performance during Transesterification reaction of vegetable oils with methanol. The development of catalysts loaded on support or carrier is very promising and has shown good conversion results in this regard. Heterogeneous catalysts can be designed to give higher activity, selectivity and longer catalyst lifetime (Hillion et al., 2003). Briefly, heterogeneous catalysts such as alkali metal (Li, Na, K)-promoted alkaline earth oxides (CaO, BaO, MgO), as well as K_2CO_3 supported on (Al_2O_3), have been used for Transesterification of Canola oil with molar ratio of alcohol to oil of 11.48:1, catalyst loading of 3.16 wt%, at 60 °C., for 2 h with more than 85% conversion. Also, Transesterification of unrefined or waste oil over lanthanum-promoted zinc oxide ($ZnO-La_2O_3$) catalysts, with a 3:1 ratio of zinc to lanthanum, at 170–220 °C, 126 g of oil, 180 g of methanol, and 3 g of catalyst gave over 96% in 3 h (Yan et al., 2009). Others include KNO_3/Al_2O_3 (Vyas et al., 2009), La_2O_3/ZrO_2 (Sun et al., 2010), K_2CO_3 on alumina/silica support (Lukic et al., 2009) and KNO_3/KL zeolite and KNO_3/ZrO_2 (Jitputti et al., 2006).

In this study, we describe the performance of supported Mg-Zn on activated carbon (AC) for the Transesterification of WFO with methanol. To obtain maximum conversion for the process, different reaction parameters such as WFO to methanol molar ratio, reaction temperature, catalyst loading, and reaction time were studied. The activated

carbon is chosen due to its high porous structure as well as low cost compared to conventional supports such as alumina and silica. Structural, functional and surface chemistry of the prepared catalyst were performed. Moreover, the catalyst reuse and stability were elucidated.

2. METHODOLOGY

2.1. Chemicals

Waste frying oil (WFO) was obtained from the University of Science, Malaysia cafeteria. The properties of the oil such as kinematic viscosity, acid value and density were determined as $3.65 \times 10^{-4} m^2 s^{-1}$, 2.02 mg KOH g^{-1} oil and $891 kg m^{-3}$, respectively. Others are the average refractive index over three determinations, 1.47, moisture content, 0.09% and shear stress, 7.98 N/m². Analytical grade of KOH (>85%), $Mg(NO_3)_2 \cdot 6H_2O$ (>99%), $Zn(NO_3)_2 \cdot 6H_2O$ (>98%), KNO_3 (99%), used to synthesize the catalysts were purchased from Sigma–Aldrich Pty Ltd., Malaysia. Analytical reagent grade 99.9% methanol (HPLC) purchased from Merck (Malaysia) was used for the Transesterification reactions. The reference standards which are methyl stearate (>99.5%), methyl palmitate (>99.5%), methyl myristate (>99.5%), methyl oleate (>99.5%) and methyl linoleate (>99.5%) as well as methyl heptadecanoate (99.5%) used as internal standard for gas chromatography (GC) analysis was purchased from Sigma–Aldrich (Malaysia) and n-hexane (96%) used as solvent for GC analysis was purchased from MERCK, (Malaysia). All the chemicals used were analytical reagent grade.

2.2. Preparation of catalyst

Activated carbon supported Mg-Zn oxides was prepared by co-precipitation and impregnation of the AC with an equimolar (0.5 M) aqueous solution of the nitrates of Magnesium, $Mg(NO_3)_2 \cdot 6H_2O$ and zinc, $Zn(NO_3)_2 \cdot 6H_2O$ which was used as precursor for Mg-Zn oxides. The



www.seetconf.futminna.edu.ng



www.futminna.edu.ng

equimolar solution of Mg-Zn was precipitated with 4 M solution of ammonia water. The activated carbon used has previously been prepared and characterized and was used without any pretreatment. The solution mixture was stirred for 3 h at 60 °C to homogenize. The catalyst was obtained by loading constant amount of AC support, 100 g for each batch preparation, to the precursor under constant agitation. After impregnation, the sample was allowed to age for 12 h before it was oven dried for 24 h at 100 °C. This was followed by calcinations in a furnace at the temperature 500 °C for 4 h.

2.3. Catalyst characterization, activity testing, and evaluation of methyl ester content

The synthesized catalyst samples were characterized by elemental analyzer using an energy dispersive X-ray detector (EDX) mounted on the microscope and Philips XL30S model Scanning Electron Microscope (SEM), X-ray powder diffraction analysis was conducted on a diffractometer, model Philips PW1710, with Cu K α radiation at 40 kV and 40 mA. The surface areas and textural characteristics of the prepared catalysts were determined using the Brunauer Emmett Teller (BET) method. The data were acquired on Micromeritics ASAP2020 adsorption analyzer (Micromeritics instruments corporation, USA) at -197°C. Fourier transform infrared spectroscopy (FTIR) was used to qualitatively identify the chemical functionality of the catalysts. FTIR spectra were recorded between 4000 and 400 cm⁻¹. Scanning Electron Microscopy (SEM) analysis was carried out to study the textural morphologies of the as-synthesized catalysts. Gas chromatography GC-2010 plus (Schimadzu, Japan) supplied by Fischer Scientific (M) Sdn, Bhd with Flame ionization detectors (FID-2010 plus) and split/split less injection unit (SPL-2010 plus) equipped with a capillary column (Nukol30 m x 0.53 mm x 1 μ m) was used for sample analysis. Helium was used as the carrier gas. The injection was performed in split mode with a split ratio of

100:1. The analysis of methyl ester yield for each sample was carried out by dissolving 20 μ L of FAME into 250 μ L methyl heptadecanoate which was used as internal standard to give a dilution factor of 14.1 μ L of the prepared solution sample was withdrawn and injected into the GC and the methyl ester yield was calculated using appropriate standards and methods for GC calibration and analysis (Munari et al., 2007).

2.4. Transesterification of waste frying oil with methanol

Prior to charging WFO into the reactor, it was filtered with a fine screen cloth to remove impurities such as food bits and sludge. The oil was pretreated by heating at 80°C for 1 h to separate adhered water and volatile food particles. A 300 mL stainless steel batch reactor PARR 4842 from Autoclave Engineers equipped with a stirrer, thermocouple and a pressure device surrounded by a heating mantle controlled by a proportional integral derivative (PID) temperature controller was used for the Transesterification reaction. A measured quantity of

the pretreated oil and methanol in the desired ratio were charged into the reactor containing the catalyst. The reactor contents were kept under constant stirring at maximum speed to avoid mass transfer limitations. Similarly, the stirring commenced immediately at the start of the reaction to allow sufficient contact between the participating species and was maintained throughout the duration of the reaction. In a particular batch experiment with the WFO, 52 g oil was measured and charged into the reactor with 17 g of methanol equivalent to a molar ratio of methanol to oil of 9:1 was used with 2.5 wt% catalyst (1.317 g) based on oil at a temperature of 120°C.

2.5 Catalyst stability

The possibility of reusing the catalyst was investigated to check its capacity to provide the same performance during Transesterification reaction. To achieve this, the supported

catalyst was recovered after first run, washed with n-hexane to remove oil adhered to its surface, filtered and oven dried 70°C for 12 h. It was then used in the second experimental run and the procedure was repeated for the third and fourth runs for methyl ester synthesis by Transesterification reaction between methanol and WFO.

3. RESULTS AND DISCUSSIONS

3.1. Catalyst characterization

The textural properties of any catalyst are important features that provide insights as concerns its performance. To this effect, BET surface area, average pore size, and pore volume of the catalyst were determined as 91.44 m²/g, 8.52 nm, and 0.19 cm³/g, respectively. The external surface area of the as-synthesized catalyst was observed to favour its reactivity. In this study, AC support helped to improve the surface area of the catalyst forming a composite structure with Mg-Zn oxides. The surface of the AC used is comprised of well pronounced and orderly pores developed over the surface after activation. A typical SEM image for one of the synthesized catalyst is as shown in Fig.1. It was observed that there was agglomeration of particles on the surface over the AC support. The AC layer seems to be embedded due to the precursor which penetrates the support. It was also observed that the penetration into the support was inhomogeneous and was at least a few micrometers in depth with few porous opening. The exhibited nature is as a result of different materials made up of AC and the precursors integrated together consisting of particles that are not all of the same degree or dimensions. It was also observed that for a fixed concentration of the precursor, a continuous flat layer was obtained. The layer, however, covered the rough AC support yielding a thin film. It was also observed that the agglomerates of particles consisting of the precursor oxides synergized together in a composite matrix. The presence of the metals is also

confirmed by the XRD measurements which revealed that the metals are dispersed on the specific sites which could be responsible for the high performance of the as-synthesized catalyst.

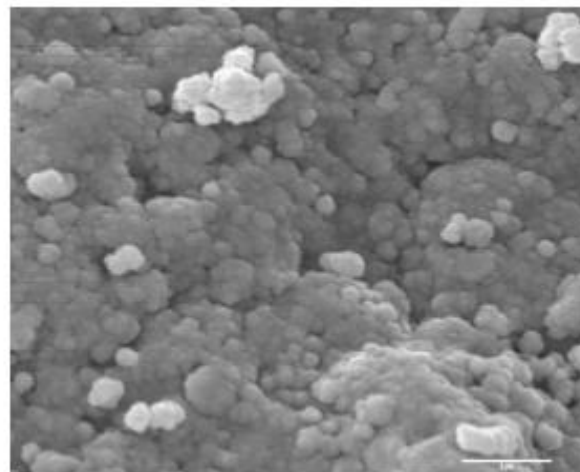


Fig.1 Scanning electron micrograph (SEM) image of Mg-Zn on AC support

The specific surface area and pore volume of the catalyst was analyzed using nitrogen adsorption at -197°C. As shown in the adsorption isotherms of Fig.2, monolayer formation was usually complete when the relative pressure reached 0.3 because the radius available for condensation was decreased by the thickness of the monolayer or by approximately two molecular diameters. Based on the results, the samples with relative pressures above 0.3 had type IV hysteresis according to the IUPAC classifications, indicating the presence of mesoporous materials related to cylindrical pores. The relative pressure versus volume adsorbed for the catalyst with a steep increase in the isotherm of the amount of N₂ adsorbed corresponds to the filling of micro pore with N₂, this is followed by the nearly horizontal adsorption and desorption branches. The inter-crystalline textural porosity was indicated at high relative pressure (P/P₀ = 0.99) as revealed by the observed hysteresis loop.

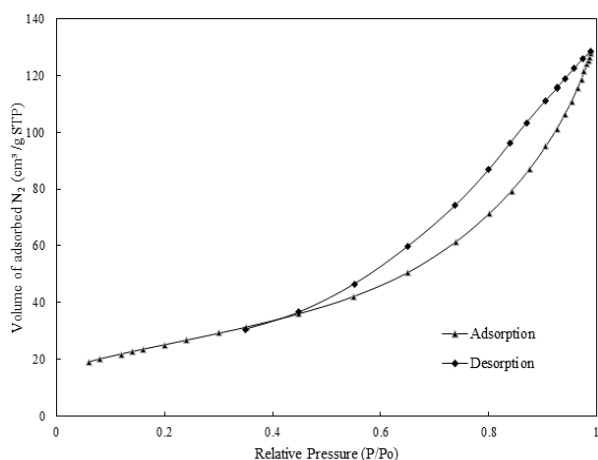


Fig. 2 Adsorption-desorption isotherms for Mg-Zn/AC catalyst sample calcined at temperature

500 °C and time of 4 h

The FTIR spectra of the used and fresh catalyst are shown in Fig. 3. The spectra show similar active surface functional groups in the region 3300–3550 cm^{-1} that represents the O–H stretching vibrations including hydrogen bonding in water molecules. Other peaks detected are found at bandwidths of 1620–1560 cm^{-1} that is vibration of surface hydroxyl groups attached to the metals and undissociated water molecules forming the surface hydrated layer. However, there are distinct differences between the catalysts spectra in the region 1150–420 cm^{-1} . The peaks at 2925 and 2860 are ascribed to C-H aliphatic stretching. Other important peaks at 1030 cm^{-1} and 1100–1120 cm^{-1} represent C-O stretching. The peaks of symmetrical stretching of C=C are also observed at 1614–1699 cm^{-1} . It was observed at 1385 cm^{-1} a peak which could be due to the presence of $-\text{CH}_3$ stretching. The intensity of peak at 2925 and 2860 cm^{-1} , 1100–1120 cm^{-1} were decreased due to the intensities in the interaction between the precursor and the activated carbon. The band sat 1150–920 cm^{-1} could be ascribed to M–O–H stretching vibrations, whereas those

between 580 and 500 cm^{-1} are assigned to M–O bending vibrations. These observations could be due to the different interaction of the precursor's oxides on the activated carbon. The peaks for the both spectra are assigned based on existing data from literature (Miller and Wilkins, 1952). The spectra of both catalysts are found to be similar in all respect but for some new peaks established.

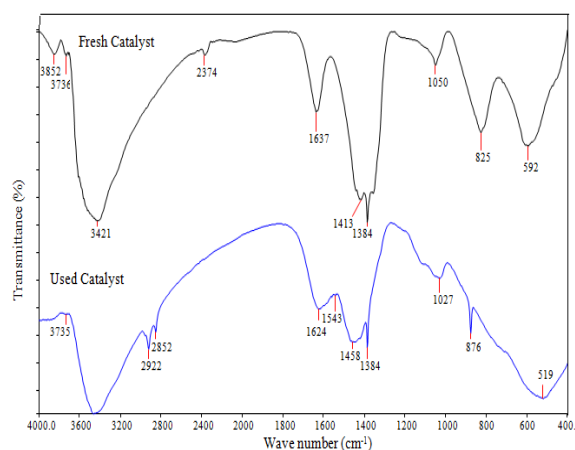


Fig.3 FTIR spectra analysis for the fresh and used Mg-Zn/AC catalyst

XRD analysis was performed in order to identify the crystalline phases present in the Mg-Zn/AC catalyst. The diffractograms for fresh and 3rd cycle reused samples is as shown in Fig. 4. The sample calcined at 500 °C for 4 h exhibited the XRD peaks at $2\theta = 30^\circ$, 50.6° and 60.3° (strong) assigned to the tetragonal phase. It also showed weak XRD peaks at $2\theta = 34^\circ$,

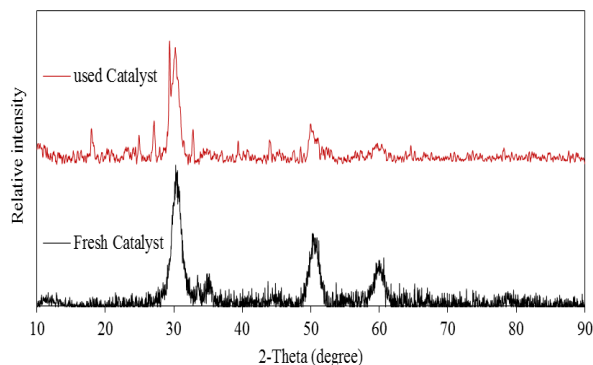


Fig. 4 XRD spectra for the fresh and used Mg-Zn/AC catalyst

35.8°, and 78° assigned to the monoclinic phase. The presence of both phases is responsible for the observed catalytic activity. Magnesium has strong intensity at $2\theta = 30^\circ$ while other peaks are weakly dispersed. The EDX analysis was used to characterize the catalyst and the results of the analyzed samples are presented Fig.5. The spectra clearly showed the existence of Zn, Mg, and C with prominent peaks and the elemental composition further revealed the presence of carbon as the source of activated carbon used for the support with the value is as high as 15.26 wt%. The composition of the catalyst was verified by using an EDX mounted on the microscope and the elemental analysis revealed that the sample contained 10.12 wt% K, 28.03 wt% Zn, 11.28 wt% Mg and 35.31 wt% O. This was in good agreement with the XRD diffractograms

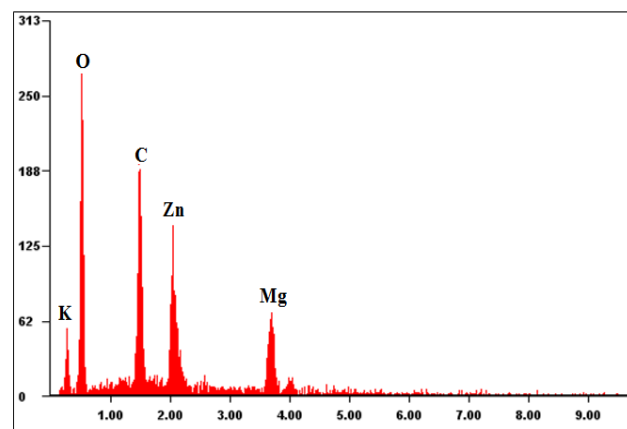


Fig.5 Energy dispersive X-ray (EDX) spectra of the Mg-Zn/AC catalyst

3.2 Thermal Gravimetric Analysis (TGA)

The thermal stability of the catalyst given in Fig.6 was studied via thermal gravimetric analysis in oxygen at a heating rate 10°C/min in the range of 34- 800°C. The thermal gravity curve showed that the synthesized compound had a weight loss of approximately 46.25% between 190°C and 486°C. This corresponds to the decomposition of the organic component of the activated carbon and the metal oxide layers. When the temperature is increase over 480 °C, an increase in mass was observed, which could be attributed to the oxidation of metal precursors as the compound transforms into crystalline oxides.

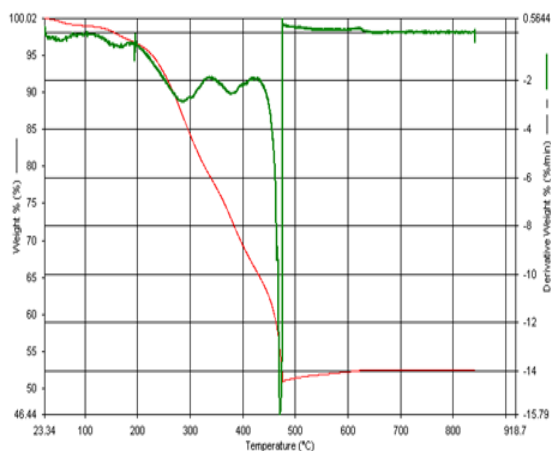


Fig.6 Thermal gravimetric analysis of the Mg-Zn/AC catalyst at a flow of 60 cm³/min of N₂

and a heating rate of 10 °C/min from 34 °C to 800 °C

3.3 Heat treatment effect on MgZnO/AC catalyst and test of performance

The catalyst was subjected to different calcinations temperatures in the range of 300-700°C for 4 h and the activity was examined on the Transesterification of waste frying oil with methanol. As shown in Fig. 7, the performance of the catalyst increased as the calcinations temperature is increased. This can be explained by the fact that the precursors undergo phase transition as the temperature is increased, and this is supported by the XRD and the TGA analysis where crystalline formation of MgZnO, MgO and ZnO existed in the specified range. The phase transformation could have resulted due to the basic character of the catalyst which provides a favourable condition for Transesterification of low free fatty acid oil feedstock. FAME content of above 84% was obtained with the catalyst calcined at 500 °C and a decrease in the catalyst

performance was observed when it was calcined above this temperature. The reason could be due to sintering at temperature > 500 °C as observed in the TGA analysis where further increase in temperature is no longer economical for Transesterification. Therefore, 500 °C was chosen as the calcinations temperature and was employed in the subsequent experimental runs.

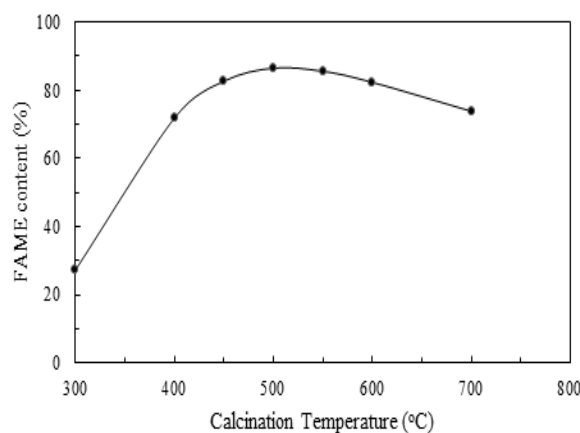


Fig.7 Yield of methyl esters at different calcined temperatures

3.4 Effect of reaction time

Reaction time is an important factor that during Transesterification reaction. The diffusion and mass transfer limitations of heterogeneous catalyst result to slow reaction and the stirrer speed was set to maximum to overcome the mass transfer limitations. Thus, at the commencement of the reaction, the FAME content was low during 1 h of reaction. However, Fig. 8 shows that the FAME content increased gradually after 2 h of reaction time, and thereafter remained nearly constant at 84% during 5 h reaction time. It was also observed that further increase in time up to 12 h produced no significant change to the FAME content rather a slight decrease was noticed as the reaction time was extended with FAME content of 78%. This observation could be as a result of a backward shift in the

reaction being a reversible process; the reaction complex formed at this extended period no longer favoured the yield of methyl esters.

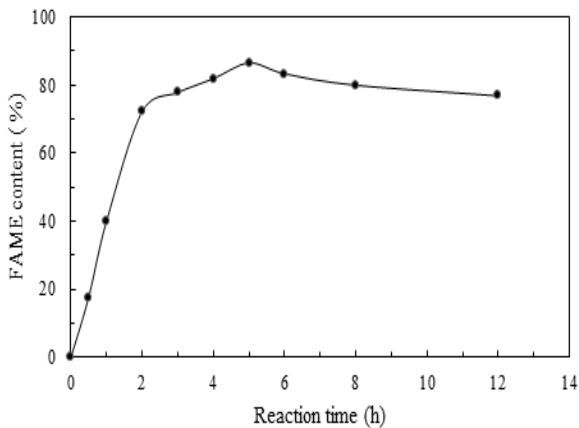


Fig.8 Yield of methyl esters at different reaction time

3.5 Effect of catalyst loading

The effect of catalyst dosage on the yield of esters was investigated with the amount of catalyst varied in the range 0.5-6.5 wt% (catalyst to oil). Fig. 9 show that FAME content increased gradually (> 84%) with the increment of catalyst to oil weight ratio from 0.5 to 2.5 wt%. After that, the FAME content started to decrease with further addition of catalyst amount. The observed trend could be due to resistant of mixing involving triglyceride molecules, product and solid catalyst in which case the viscosity increased as the catalyst loading was increased Thus, a good value of 2.5 wt% was found suitable for high FAME content in this process.

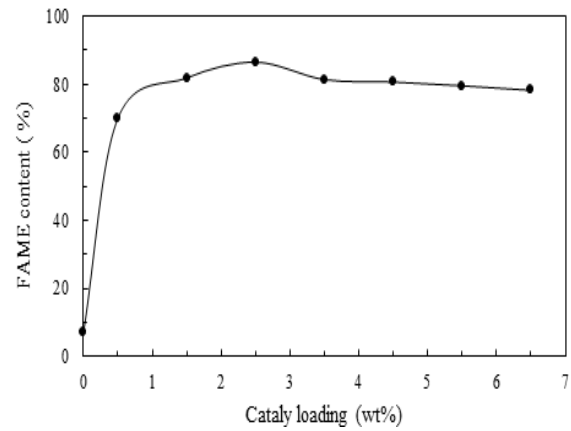


Fig.9Yield of methyl esters at different catalyst loading

3.6 Effect of methanol to oil molar ratio

Transesterification reaction requires stoichiometrically, three moles of methanol to one mole of triglyceride. To shift the reaction forward, an excess of methanol to oil ratio is needed. It was observed from Fig. 10 that FAME content increase as expected, up to a maximum value of 86%. Beyond this point, as the ratio of alcohol to oil was further increased, there was a decline in the FAME content. The observed decrease in yield as the alcohol-oil ratio was increased could be due to dilution effect caused by the excess methanol making the separation difficult and also reduce the catalyst concentration.

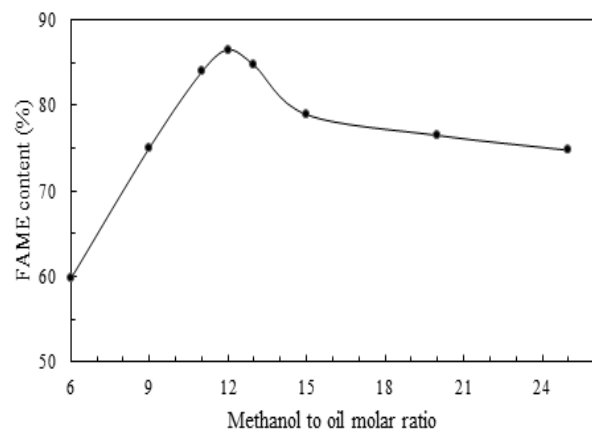


Fig. 10 Yield of methyl esters at different methanol to oil molar ratio

3.7 Effect of reaction temperature

The effect of the reaction temperature was investigated in the range of 70-180 °C. During the preliminary runs reaction temperature below 70 °C produced methyl esters lower than 55% which increased to more than 76% at a higher temperature of 120 °C. The highest ester content was obtained at 150 °C as shown in Fig.11. From a kinetic performance, reaction rate is expected to increase with increase in temperature because an increase in collision among molecules lowers the activation energy barrier resulting in more product conversion. However, in this study, at higher temperature beyond 150 °C, a decrease in FAME content was obtained, an indication of temperature inhibiting effect of the catalyst which affects its activity during the Transesterification reaction. Thus, 150 °C was chosen as a suitable operating temperature in this study.

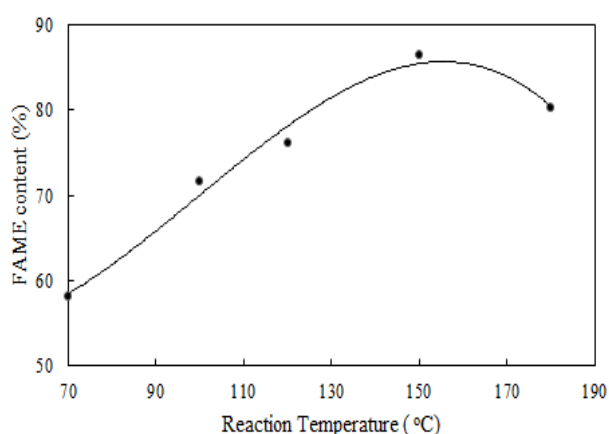


Fig. 11 Yield of methyl esters at different reaction temperature

3.8 Catalyst stability during Transesterification

The reusability was examined after the first run. After the first run, the catalyst was filtered from the product and was washed with n-hexane until all adhered oil and glycerol were removed, then it was dried at 70°C for 12 h and was placed in contact with fresh methanol and WFO for the next run. The result of the catalyst performance during reusability test is shown in Fig. 12. It can be seen from the profile that the yield of ester decreased with increase in the experimental runs. Yields of 86% ester was obtained at first run, while the second, third and fourth runs resulted in 80%, 70%, and 58% of esters, respectively. The result could be due to deactivation of the active sites as a result of clogging by some triglyceride molecules. Also, the observed decrease could be due to loss of material during manipulation which resulted in fewer active sites of the catalyst for the Transesterification reaction in subsequent runs.

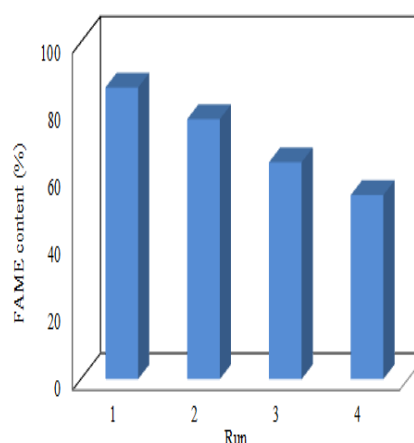


Fig. 12 Yield of methyl esters at different runs during stability studies

4. CONCLUSION

The MgZnO/AC supported catalyst was synthesized by incipient wetness impregnation method and was used in Transesterification of



www.seetconf.futminna.edu.ng



www.futminna.edu.ng

waste frying oil. The catalyst showed good activity towards the synthesis of methyl esters with optimum conditions obtained at methanol to oil molar ratio of 12:1, catalyst loading 2.5 wt%, temperature 150 °C, and reaction time 5 h to give over 86% yield methyl ester when the catalyst was calcined at 500 °C for 4h. Catalyst separation from the product mixture is simple and reusable for three cycles. The current investigation showed that Mg-Zn/AC catalyst presented efficient activity during the Transesterification reaction of WFO and could be a promising heterogeneous catalyst for the production biodiesel fuel from other vegetable oil feedstock.

REFERENCE

- Al-Zuhair, S., 2007. Production of biodiesel: possibilities and challenges. *Biofuels*
- Bioprod.Biorefin.*1, 57– 66.
- Cheng, H.F., Hu, Y.N., 2010. Municipal solid waste (MSW) as a renewable source of energy: Current and future practices in China. *Bioresour.Technol.* 101, 3816-3824.
- D'Cruz, A., Kulkarni, M.G., Meher, L.C., Dalai, A.K., 2007. Synthesis of biodiesel from canola oil using heterogeneous base catalyst. *J. Am. Oil Chem. Soc.* 84, 937–943.
- Furuta, S., Matsushashi, H., Arata, K., 2004. Biodiesel fuel production with solidsuperacid catalysis in fixed bed reactor under atmospheric pressure. *Catal.Commun.* 5, 721–723.
- Gnansounou, E., Dauriat, A., 2010. Techno-economic analysis of lignocellulosic ethanol: A review. *Bioresour.Technol.* 101, 4980-4991.
- Granados, M.L., Poves, M.D.Z., Alonso, D.M., Mariscal, R., Galisteo, F.C., Moreno-Tost, R., Santamaria, J., Fierro, J.L.G., 2007. Biodiesel from sunflower oil by using activated calcium oxide. *Appl. Catal. B: Environ.* 73, 317–326.
- Hillion, G., Delfort, B., Pennec, D., Bournay, L., Chodorge, J., (2003). Biodiesel production by a continuous process using a heterogeneous catalyst. *American Chemical Society, Division Fuel Chemistry.* 48 (2), 636-638
- Jitputti, J., Kitiyanan, B., Rangsunvigit, P., Bunyakiat, K., Attanatho, L., Jenvanitpanjakul, P., 2006. Transesterification of crude palm kernel oil and crude coconut oil by different solid catalysts. *Chem. Eng. J.* 116, 61–66.
- Kim, H.-J., Kang, B.-S., Kim, M.-J., Park, Y.M., Kim, D.-K., Lee, J.-S., Lee, K.-Y., 2004. Transesterification of vegetable oil to biodiesel using heterogeneous base catalyst. *Catal. Today* 93–95, 315–320.
- Lukic, I., Krstic, J., Jovanovic, D., Skala, D., 2009. Alumina/silica supported K₂CO₃ as a catalyst for biodiesel synthesis from sunflower oil. *Bioresour.Technol.* 100, 4690–4696.



www.seetconf.futminna.edu.ng



www.futminna.edu.ng

- MacLeod, C.S., Harvey, A.P., Lee, A.F., Wilson, K., 2008. Evaluation of the activity and stability of alkali-doped metal oxide catalysts for application to an intensified method of biodiesel production. *Chem. Eng. J.* 135, 63–70.
- Miller, F. A. and Wilkins, C.H., (1952). Infrared Spectra and Characteristic Frequencies of Inorganic Ions. *Analytical Chemistry*. 24 (8), 1253-1294
- Munari, F., Cavagnino, D., Cadoppi, A., 2007. Determination of Total FAME and Linolenic Acid Methyl Ester in Pure Biodiesel (B100) by GC in Compliance with EN14103. Thermo Fisher Scientific, Milan, Italy.
- Ong, H.C., Mahlia, T.M.I., Masjuki, H.H., 2011. A review on energy scenario and sustainable energy in Malaysia. *Renewable Sustainable Energy Rev.* 15, 639-647.
- Singh and Singh, (2010). Biodiesel production through the use of different sources and characterization of oils and their esters as the substitute of diesel: A review. *Renewable and Sustainable Energy Reviews*. 14, 200-216
- Sun, H., Ding, Y., Duan, J., Zhang, Q., Wang, Z., Lou, H., Zheng, X., 2010. Transesterification of sunflower oil to biodiesel on ZrO_2 supported La_2O_3 catalyst. *Bioresour. Technol.* 101, 953–958.
- Suppes, G.J., Dasari, M.A., Daskocil, E.J., Mankidy, P.J., Goff, M.J., 2004. Transesterification of soybean oil with zeolite and metal catalysts. *Appl. Catal. A: Gen.* 257, 213–223.
- Vyas, A.P., Subrahmanyam, N., Patel, P.A., 2009. Production of biodiesel through transesterification of Jatropha oil using KNO_3/Al_2O_3 solid catalyst. *Fuel* 88, 625–628.
- Yan, S., Salley, S. O. and Simon Ng, K.Y., (2009). Simultaneous transesterification and esterification of unrefined or waste oils over $ZnO-La_2O_3$ catalysts. *Applied Catalysis A: General*. 353 (2), 203-212
- Yin, S.D., Dolan, R., Harris, M., Tan, Z.C., 2010. Subcritical hydrothermal liquefaction of cattle manure to bio-oil: Effects of conversion parameters on bio-oil yield and characterization of bio-oil. *Bioresour. Technol.* 101, 3657-3664.
- Yung B.C., Gon S., 2010. High activity of acid-treated quail eggshell catalysts in the transesterification of palm oil with methanol. *Bioresour. Technol.* 101, 8515-8519.
- Zabeti, M., Daud, W.M.A.W., Aroua, M.K., 2009. Optimization of the activity of CaO/Al_2O_3 catalyst for biodiesel production using response surface methodology. *Appl. Catal. A: Gen.* 366, 154–159.
- Zhang, Z.Y., Qu, W.W., Peng, J.H., Zhang, L.B., Ma, X.Y., Zhang, Z.B., Li, W., 2009. Comparison between microwave and conventional thermal reactivations of spent activated carbon generated from vinyl acetate synthesis. *Desalination*. 249, 247-252.